

Research Article

Open Access



Robust coverage control of multiple USVs with time-varying disturbances

Qihai Sun¹, Zhi-Wei Liu^{2,3}, Ming Chi^{2,3}, Ming-Feng Ge⁴, Dingxin He^{2,3}

¹China Ship Development and Design Center, Wuhan 430064, Hubei, China.

²School of Artificial Intelligence and Automation, Huazhong University of Science and Technology, Wuhan 430074, Hubei, China.

³Key Laboratory of Image Processing and Intelligent Control, Ministry of Education, Huazhong University of Science and Technology, Wuhan 430074, Hubei, China.

⁴School of Mechanical Engineering and Electronic Information, China University of Geosciences, Wuhan 430074, Hubei, China.

Correspondence to: Prof. Zhi-Wei Liu, School of Artificial Intelligence and Automation, Huazhong University of Science and Technology, No. 1037, Luoyu Road, Wuhan 430074, Hubei, China. E-mail: zwliu@sina.com

How to cite this article: Sun Q, Liu ZW, Chi M, Ge MF, He D. Robust coverage control of multiple USVs with time-varying disturbances. *Intell Robot* 2023;3(3):242-56. <http://dx.doi.org/10.20517/ir.2023.15>

Received: 17 Mar 2023 **First Decision:** 10 May 2023 **Revised:** 22 May 2023 **Accepted:** 2 Jun 2023 **Published:** 20 Jul 2023

Academic Editor: Simon X. Yang, Anh-Tu Nguyen **Copy Editor:** Yanbin Bai **Production Editor:** Yanbin Bai

Abstract

This paper investigates the problem of optimal coverage control for multiple unmanned surface vehicles (USVs) in the presence of time-varying disturbances. To solve this problem, the disturbance vector observer is designed to approximate the unknown time-varying disturbances. It is demonstrated that the estimated disturbance vector converges to the actual disturbance vector within a finite time. To achieve the optimal coverage effect of the task region, the control idea of layer-by-layer design is borrowed, and the desired velocities of the USV are designed. By following the desired velocities, the USV network can achieve the optimal coverage effect of the task region. Based on the estimated disturbances, a robust coverage controller is designed to achieve the tracking of desired velocities by the USV within a finite time, ultimately achieving optimal coverage effect of the task region by the USV network. Finally, corresponding simulation results are provided to validate the effectiveness of the proposed approach.

Keywords: Coverage control, disturbance observation, multiple unmanned surface vehicles, finite time control



© The Author(s) 2023. **Open Access** This article is licensed under a Creative Commons Attribution 4.0 International License (<https://creativecommons.org/licenses/by/4.0/>), which permits unrestricted use, sharing, adaptation, distribution and reproduction in any medium or format, for any purpose, even commercially, as long as you give appropriate credit to the original author(s) and the source, provide a link to the Creative Commons license, and indicate if changes were made.



1. INTRODUCTION

With advancements in technology and theoretical progress in multi-agent systems, multi-agent cooperative control has gained popularity in both military and civilian applications. One of the key research areas in this field is multi-agent system coverage control within a designated task region. The coverage control problem has a wide range of practical applications, including environmental monitoring, search and rescue missions, harbor patrolling, and area defense. As a result, researchers have dedicated considerable attention to addressing this problem in recent decades^[1-7].

The coverage control problem poses a common challenge in deploying an agent network within a task region to optimize task execution. One widely used approach for addressing this problem is based on Voronoi partition, which was first proposed in the work of Ref.^[8]. Since then, numerous scholars have conducted extensive research on the coverage control problem using Voronoi partition. For example, Ref.^[9] solved the coverage control problem concerning the deployment of mobile sensor networks in non-convex domains. Meanwhile, Ref.^[5] studied the coverage control problem for non-convex regions, taking into account the heterogeneity of sensing range in mobile robot networks. In the research presented by Ref.^[10], a coverage control strategy for mobile sensor networks with limited communication range was proposed, where the trajectory of the robots is constrained to a circle. Additionally, Ref.^[11] proposed a region coverage control law for a team of first-order kinematic model mobile robots operating within a two-dimensional region with time-varying risk density.

In view of the presence of unknown information in the coverage control problem, several scholars have proposed adaptive coverage control methods to optimize the coverage efficiency^[12-14]. In the work of Ref.^[12], the unknown density function is approximated using the feedforward neural network method, followed by a coverage control algorithm for the sensor network based on this approximation. An observer is introduced to estimate the unknown information in Ref.^[13], and a controller is designed to achieve optimal coverage effects. Additionally, in Ref.^[14], a multi-agent coverage control law with time-varying model uncertainty is proposed, utilizing function approximation techniques.

It is worth noting that the kinematic model of the agent used in the above coverage control studies is the first-order integral model^[5-14] or the second-order model^[4]. However, the agent typically exhibits underactuated characteristics in practical applications, and designing a controller for underactuated agents can present additional challenges. To address this issue, Ref.^[15] proposed gradient-descent coverage control algorithms for underactuated wheeled vehicles. Meanwhile, Ref.^[16] proposed an observer-based coverage control law for a unicycle multi-agent network with external disturbance in a dynamic environment. The swarm-based coverage control in Ref.^[17] considers two different types of agents: the unicycle agent and the single-integrator agent. However, in practical scenarios such as ocean environmental monitoring, marine scientific research, and marine security defense^[18-20], the underactuated unmanned surface vehicle (USV) is widely used, which has stronger underactuated characteristics and operates in complex working environments. The agent models considered in the aforementioned studies on area coverage control are relatively simple models, and their proposed control laws cannot be directly applied to the USV model. As a result, there is currently limited research on marine area coverage control of the USV. In the application of USV control, the movement of USVs is frequently affected by the marine environment, and disturbances generated by the marine environment may prevent the movement of the USV from achieving the desired performance. Therefore, it is necessary to take into account the impact of unknown disturbances. Considering the influence of model uncertainties and environmental disturbances, Ref.^[21] and Ref.^[22] proposed path following strategies for the USV based on robust neural damping adaptive methods and the fuzzy logic system, respectively. Addressing time-varying delay and uncertainty topology, Ref.^[23] studied the consensus problem among agents operating under Markov switching topology. With a focus on the network security and uncertainty, Ref.^[24] studied the elastic consensus problem of dynamic network agents based on the media consensus strategy. Considering bounded uncertainties and external disturbances, Ref.^[25] proposed an adaptive control strategy for the super-twisting controller to

achieve trajectory tracking of USVs. In the presence of disturbances, a fixed time line of sight (LOS) guidance law and a fixed time heading controller based on the fixed time disturbance period are proposed in Ref. [26] to drive the USV to track the expected path within a fixed time frame.

This paper investigates the coverage control problem for the USV network in the presence of unknown time-varying disturbances. To address this challenge, the disturbance vector observer is designed to estimate time-varying disturbances. Subsequently, the coverage controller is developed based on the observer to guide each USV to track desired velocities. Furthermore, the optimal location configuration of the USV network is implemented to optimize the coverage of the task region.

The paper is structured as follows. Section II presents the simplified kinematic and dynamic models of the USV, along with an overview of the coverage control problem. Next, in Section III, the design of expected velocities for USVs is discussed, and it is demonstrated that optimal coverage of the task region can be achieved by utilizing these velocities. Subsequently, Section IV details the design of a finite-time disturbance observer, which aims to estimate external input disturbances. Using the observer, a control law is then developed to drive the velocities of USVs toward the desired values within a finite time. Lastly, Sections V and VI present simulation results and conclusions, respectively.

2. PROBLEM FORMULATION

The USV set \mathcal{V} , which consists of n USVs ($\mathcal{V} = \{1, 2, \dots, n\}$), is considered in a task region $Q \in R^2$. The kinematic model of the USV can be described as

$$\begin{bmatrix} \dot{x} \\ \dot{y} \\ \dot{\psi} \end{bmatrix} = \begin{bmatrix} \cos(\psi) & -\sin(\psi) & 0 \\ \sin(\psi) & \cos(\psi) & 0 \\ 0 & 0 & 1 \end{bmatrix} \begin{bmatrix} u \\ v \\ r \end{bmatrix}, \quad (1)$$

where $\eta = [x, y, \psi]^T$ are the position and the heading angle in the earth-fixed frame. $V = [u, v, r]^T$ denote the surge, sway velocities, and the angular velocity in the body-fixed frame. Considering time-varying disturbances caused by the Marine environment, the dynamics of the USV are:

$$M\dot{V} + C(V)V + D(V)V = \tau + \tau_d, \quad (2)$$

where $M = M^T \in R^{3 \times 3}$ is the inertial matrix, $C(V) \in R^{3 \times 3}$ denotes the Coriolis and centripetal matrix, and $D(V) \in R^{3 \times 3}$ denotes the damping matrix. $\tau = [\tau_u \ 0 \ \tau_r]^T$ is the control input, and $\tau_d = [\tau_{ud} \ \tau_{vd} \ \tau_{rd}]^T$ is the unknown time-varying disturbances caused by wind, waves, currents, and other factors. In order to simplify the control design of USVs, assuming that the USV is symmetric, $M = \text{diag}\{m_{11}, m_{22}, m_{33}\}$,

$$C(V) = \begin{bmatrix} 0 & 0 & -m_{22}v \\ 0 & 0 & m_{11}u \\ m_{22}v & -m_{11}u & 0 \end{bmatrix},$$

and $D(V) = \text{diag}\{d_{11}, d_{22}, d_{33}\}$. The simplified surface 3-DOF dynamic is:

$$\begin{aligned} m_{11}\dot{u} &= m_{22}vr - d_{11}u + \tau_u + \tau_{ud}, \\ m_{22}\dot{v} &= -m_{11}ur - d_{22}v + \tau_{vd}, \\ m_{33}\dot{r} &= -(m_{22} - m_{11})uv - d_{33}r + \tau_r + \tau_{rd}. \end{aligned} \quad (3)$$

The USV is equipped with an actuator module to perform the corresponding tasks. The performance of the actuator is optimal when the USV is located nearby, but it gradually weakens as the distance to be covered

increases. The performance function $f(\|q - p_i\|)$ is used to describe the performance variation for the actuator of the i -th USV [27,28],

$$f(\|q - p_i\|) = k_f \exp(-\beta \|q - p_i\|^2), \quad (4)$$

where $\|q - p_i\|$ is the 2-norm of the vector $q - p_i$, $q \in Q$ is any point within task region Q , $p_i = [x_i \ y_i]^T$ is the position of i -th USV, and $k_f, \beta > 0$ are constant coefficients.

The risk density function $\Phi(q)$ is used to quantify the importance of each point q in the task region Q

$$\Phi(q) = \phi(q) + \sum_{j=1}^m \phi(q, s_j), \quad (5)$$

where $\phi(q)$ is the constant risk density value, and $s_j = [x_j, y_j]^T$ ($j = 1, \dots, m$) represents the location of the j -th important object. $\phi(q, s_j) = \alpha_j \cdot \exp(-\frac{\|q - s_j\|^2}{2\delta_j^2})$ ($j = 1, 2, \dots, m$) is used to describe the contribution of the j -th object on risk density function $\Phi(q)$ [29,30]. $\alpha_j > 0$ is the constant coefficient. As the location point q approaches the important object s_j , the value of function $\phi(q, s_j)$ increases. Moreover, the risk density function $\Phi(q)$ evaluates the significance of a point based on its value. Therefore, higher values of $\Phi(q)$ indicate points that require greater allocation of resources for monitoring purposes.

The generalized Voronoi partition method is introduced to assign areas for each USV, as described in previous studies [8,9]. The region Q is divided according to the performance of the actuators carried by different USVs, and the i -th USV is assigned a Voronoi partition V_i

$$V_i = \{q \in Q \mid f(\|q - p_i\|) \geq f(\|q - p_j\|), i, j \in \mathcal{V}\}. \quad (6)$$

Next, the effect of USVs executing tasks within the task region Q is described. The metric function $H(P)$ is used to quantify the coverage effect of USVs on the task region Q [31,32]

$$H(P) = \sum_{i=1}^n \int_{V_i} f(\|q - p_i\|) \cdot \Phi(q) dq. \quad (7)$$

where $P = \{p_1, p_2, \dots, p_n\}$, and each USV is responsible for its Voronoi partition. The larger the value of the measurement function $H(P)$, the better the coverage effect of the USV network on the task region Q .

The goal of achieving task region coverage with the USVs is to drive the location configuration of USVs to maximize the metric function $H(P)$. If two USVs have common edges within their respective Voronoi partitions, they can establish communication with each other.

3. THE EXPECTED VELOCITIES DESIGN OF THE USVS

In this section, we will design the expected velocities of each USV to achieve optimal coverage of the task region and provide rigorous proofs to support our design.

Assumption 1 Each USV can accurately measure its position and angle information $\eta = [x, y, \psi]^T$ in the earth-fixed frame. The surge, sway velocities, and the angular velocity information $V = [u, v, r]^T$ can be obtained in the body-fixed frame through relevant sensors and other equipment. Each USV can communicate with its neighbors.

From the Voronoi partition, there is

$$H(P) = \sum_{i=1}^n H_i, \quad (8)$$

where $H_i = \int_{V_i} f(\|q - p_i\|) \Phi(q) dq$, ($i \in \mathcal{V}$).

Take the derivative of the H_i with respect to p_i

$$\begin{aligned} \frac{dH_i}{dp_i} &= \int_{V_i} \frac{\partial f(\|q-p_i\|)}{\partial p_i} \Phi(q) dq \\ &= 2 \int_{V_i} \alpha_i \beta_i f(\|q - p_i\|) \Phi(q) (q - p_i)^T dq \\ &= 2G_{vi}(C_{vi} - p_i)^T, \end{aligned} \tag{9}$$

where $G_{vi} = \int_{V_i} \alpha_i \beta_i f(\|q - p_i\|) \Phi(q) dq$, $C_{vi} = \frac{1}{G_{vi}} \int_{V_i} \alpha_i \beta_i q f(\|q - p_i\|) \Phi(q) dq$ are the generalized mass and generalized centroid of the Voronoi partition V_i .

Let

$$e_i = \begin{bmatrix} x_{ei} \\ y_{ei} \end{bmatrix} = C_{vi} - p_i, E_i = \|e_i\|, \tag{10}$$

$$\psi_{ir} = \arctan 2(x_{ei}, y_{ei}), \tag{11}$$

$$\psi_{ie} = \psi_{ir} - \psi_i. \tag{12}$$

Next, the expected velocities of the i -th USV will be designed to drive the position of the i -th USV ($i \in \mathcal{V}$) so as to optimize the coverage effect on the Voronoi partition V_i . The expected surge velocity u_d and angular velocity r_d of the USV are designed as follows:

$$\begin{cases} r_d = k_{r1} \left(\frac{1}{1+e^{-b_1 \psi_{ie}}} - \frac{1}{2} \right) + k_{r2} \psi_{ie} + \dot{\psi}_{ir}, \\ u_d = k_{u1} \left(\frac{1}{1+e^{-b_2 E_i}} - \frac{1}{2} \right) + k_{u2} E_i + \|\dot{C}_i\|, \end{cases} \quad (i \in \mathcal{V}), \tag{13}$$

where constant coefficient $k_{r1}, k_{u1} > 0$, b_1, b_2 are positive constant.

Lemma 1 ^[33] Consider the system

$$\dot{x} = f(t, x, u), \tag{14}$$

where $f : [0, \infty) \times \mathbb{R}^n \times \mathbb{R}^m \rightarrow \mathbb{R}^n$ is piecewise continuous in t and locally Lipschitz in x and u . The input $u(t)$ is a piecewise continuous, bounded function of t for all $t \geq 0$. If the unforced system $\dot{x} = f(t, x, 0)$ has a globally exponentially stable equilibrium point at the origin $x = 0$, then the system $\dot{x} = f(t, x, u)$ is input-to-state stable.

Lemma 2 ^[33] For the cascade system

$$\begin{aligned} \dot{x}_1 &= f_1(t, x_1, x_2), \\ \dot{x}_2 &= f_2(t, x_2), \end{aligned} \tag{15}$$

where $f_1 : [0, \infty) \times \mathbb{R}^{m_1} \times \mathbb{R}^{m_2} \rightarrow \mathbb{R}^{m_1}$ and $f_2 : [0, \infty) \times \mathbb{R}^{m_2} \rightarrow \mathbb{R}^{m_2}$ are piecewise continuous in t and locally Lipschitz in $[x_1, x_2]^T$. If the system $\dot{x}_1 = f_1(t, x_1, x_2)$, with x_2 as input, is input-to-stable and the origin of $\dot{x}_2 = f_2(t, x_2)$ is globally uniformly asymptotically stable, then the origin of the cascade system is globally uniformly asymptotically stable.

Theorem 1 Consider the kinematic model of the USV (0.1) with the performance function (0.4); the expected velocities (0.13) of USVs can maximize the coverage effect metric function (0.7), and the optimal coverage of the task region is achieved.

Proof Consider the following Lyapunov function

$$V_1(\psi_{ie}) = \frac{1}{2} \psi_{ie}^2. \tag{16}$$

Taking the derivative of (0.16) yields,

$$\begin{aligned}\dot{V}_1(\psi_{ie}) &= \psi_{ie} \cdot \dot{\psi}_{ie} \\ &= \psi_{ie} \cdot (\dot{\psi}_{ir} - \dot{\psi}_i) \\ &= \psi_{ie} \cdot (\dot{\psi}_{ir} - r_i).\end{aligned}\quad (17)$$

Substituting the expected angular velocity r_{id} in (0.13), it gives

$$\begin{aligned}\dot{V}_1(\psi_{ie}) &= -k_{r1} \left(\frac{1}{1 + e^{-b_1 \psi_{ie}}} - \frac{1}{2} \right) \psi_{ie} - k_{r2} \psi_{ie}^2 \\ &= -k_{r1} \left| \left(\frac{1}{1 + e^{-b_1 \psi_{ie}}} - \frac{1}{2} \right) \right| |\psi_{ie}| - k_{r2} |\psi_{ie}|^2 \\ &< -k_{r2} |\psi_{ie}|^2.\end{aligned}\quad (18)$$

It can be inferred that the error ψ_{ie} has a stable equilibrium point at the origin, which is globally exponentially stable.

Next, we define two quantities,

$$\begin{aligned}x_1 &= \psi_{ie}, \\ x_2 &= e_i^T e_i = E_i^2.\end{aligned}\quad (19)$$

Then, one has

$$\dot{x}_1 = f(t, x_1).\quad (20)$$

Taking the derivative of the quantity x_2 yields

$$\begin{aligned}\dot{x}_2 &= e_i^T (\dot{C}_{Vi} - \dot{p}_i) \\ &= e_i^T \dot{C}_{Vi} - e_i^T \dot{p}_i \\ &= e_i^T \dot{C}_{Vi} - [x_{ei}(u_i \cos \psi_i - v_i \sin \psi_i) \\ &\quad + y_{ei}(u_i \sin \psi_i + v_i \cos \psi_i)].\end{aligned}\quad (21)$$

From equation (0.12), using $\psi_{ir} - \psi_{ie}$ to replace ψ_i , one has

$$\begin{aligned}&x_{ei}(u_i \cos \psi_i - v_i \sin \psi_i) + y_{ei}(u_i \sin \psi_i + v_i \cos \psi_i) \\ &= x_{ei}(u_i \cos(\psi_{ir} - \psi_{ie}) - v_i \sin(\psi_{ir} - \psi_{ie})) + y_{ei}(u_i \sin(\psi_{ir} - \psi_{ie}) + v_i \cos(\psi_{ir} - \psi_{ie})) \\ &= x_{ei}(u_i \cos \psi_{ir} \cos \psi_{ie} + u_i \sin \psi_{ir} \sin \psi_{ie} - v_i \sin \psi_{ir} \cos \psi_{ie} + v_i \cos \psi_{ir} \sin \psi_{ie}) \\ &\quad + y_{ei}(u_i \sin \psi_{ir} \cos \psi_{ie} - u_i \cos \psi_{ir} \sin \psi_{ie} + v_i \cos \psi_{ir} \cos \psi_{ie} + v_i \sin \psi_{ir} \sin \psi_{ie}).\end{aligned}\quad (22)$$

According to equation (0.11), $\cos \psi_{ir} = \frac{x_{ei}}{E_i}$, $\sin \psi_{ir} = \frac{y_{ei}}{E_i}$, the expression yields

$$\begin{aligned}&x_{ei}(u_i \cos \psi_i - v_i \sin \psi_i) + y_{ei}(u_i \sin \psi_i + v_i \cos \psi_i) \\ &= x_{ei} \left(u_i \frac{x_{ei}}{E_i} \cos \psi_{ie} + u_i \frac{y_{ei}}{E_i} \sin \psi_{ie} - v_i \frac{y_{ei}}{E_i} \cos \psi_{ie} + v_i \frac{x_{ei}}{E_i} \sin \psi_{ie} \right) \\ &\quad + y_{ei} \left(u_i \frac{y_{ei}}{E_i} \cos \psi_{ie} - u_i \frac{x_{ei}}{E_i} \sin \psi_{ie} + v_i \frac{x_{ei}}{E_i} \cos \psi_{ie} + v_i \frac{y_{ei}}{E_i} \sin \psi_{ie} \right) \\ &= u_i \left(x_{ei} \frac{x_{ei}}{E_i} \cos \psi_{ie} + y_{ei} \frac{y_{ei}}{E_i} \cos \psi_{ie} \right) + v_i \left(x_{ei} \frac{x_{ei}}{E_i} \sin \psi_{ie} + y_{ei} \frac{y_{ei}}{E_i} \sin \psi_{ie} \right) \\ &= u_i E_i \cos \psi_{ie} + v_i E_i \sin \psi_{ie}.\end{aligned}\quad (23)$$

Note that

$$\dot{x}_2 = f(t, x_2, x_1).\quad (24)$$

For the system

$$\dot{x}_2 = f(t, x_2, 0), (x_1 = \psi_{ie} = 0), \quad (25)$$

one has

$$\dot{x}_2 = e_i^T \dot{C}_{Vi} - k_{u1} \left(\frac{1}{1 + e^{-b_2 E_i}} - \frac{1}{2} \right) E_i + k_{u2} E_i^4 - E_i |\dot{C}_{Vi}|. \quad (26)$$

Since $e_i^T \dot{C}_{Vi} \leq \|e_i^T\| \cdot \|\dot{C}_{Vi}\|$, it follows that

$$\begin{aligned} \dot{x}_2 &\leq \|e_i^T\| \cdot \|\dot{C}_{Vi}\| - k_{u1} \left(\frac{1}{1 + e^{-b_2 E_i}} - \frac{1}{2} \right) E_i \\ &\quad - k_{u2} E_i^4 - E_i |\dot{C}_{Vi}| \\ &\leq -k_{u1} \left(\frac{1}{1 + e^{-b_2 E_i}} - \frac{1}{2} \right) E_i - k_{u2} E_i^4 \\ &< -k_{u2} x_2. \end{aligned} \quad (27)$$

The globally exponentially stable equilibrium point lies at the origin for the system $\dot{x}_2 = f(t, x_2, 0)$. Based on Lemma (1), it can be inferred that the system $\dot{x}_2 = f(t, x_2, x_1)$ is input-to-state stable.

As the system $\dot{x}_1 = f(t, x_1)$ exhibits global exponential convergence, it can be concluded that the cascade system (x_1, x_2) is globally uniformly asymptotically stable according to Lemma (2). This suggests that $\lim_{t \rightarrow \infty} e_i = 0, (i \in \mathcal{V})$.

Because $\frac{dH_i}{dp_i} = 2G_{Vi}(C_{Vi} - p_i)^T$, it can be noted that if the position p_i of the i -th USV is located at the generalized centroid C_{Vi} of its Voronoi partition $V_i(e_i = 0)$, there are $\frac{dH_i}{dp_i} = 0$ and the i -th USV achieves the optimal coverage of partition $V_i (i \in \mathcal{V})$. When each USV achieves the optimal coverage of its respective Voronoi partition, the USV network attains the optimal coverage effect of the task region Q .

Remark 1 It can be shown that the quantity $\|\dot{C}_{Vi}\|$ exists and is bounded, and the quantity ψ_{ir} exists and is bounded when $E \neq 0$. The quantity ψ_{ir} has a singularity at $E = 0$. At the singularity, $E = 0$, the USV has achieved optimal coverage.

4. THE ROBUST COVERAGE CONTROL LAW FOR USVS

This section presents the design of an observer that can estimate the unknown time-varying disturbances of the USV within a finite time. Subsequently, a controller is designed based on the observer to drive the velocities of the USV to track the desired velocities (0.13) within a finite time.

Assumption 2 The first time derivative of the unknown time-varying disturbances $\tau_d = [\tau_{ud} \ \tau_{vd} \ \tau_{rd}]^T$ are bounded ($\|\dot{\tau}_d\| < B$).

Lemma 3 ([34]) Consider the nonlinear system (y_1, y_2) . If the system satisfied the following equations:

$$\begin{cases} \dot{y}_1 = -b_1 |y_1|^{\frac{1}{2}} \text{sign}(y_1) + y_2, \\ \dot{y}_2 = -b_2 \text{sign}(y_2 - y_1) + \delta, \end{cases} \quad (28)$$

where $b_1 > 0, b_2 > 0$, and δ is a bounded quantity. Then the system will converge to the origin and stabilize within a finite time.

Considering the dynamic model (0.3), the control input $\tau = [\tau_u \ 0 \ \tau_r]^T$ is designed to drive the velocities of the USV tracking the desired velocities (0.13) under the unknown time-varying disturbances $\tau_d = [\tau_{ud} \ \tau_{vd} \ \tau_{rd}]^T$.

It is worth noting that the designed control input τ can achieve the convergence of the velocities tracking error within a finite time.

First, the observer is designed to approximate the unknown external disturbance τ_d . Let

$$D(V) = \begin{bmatrix} m_{22}vr - d_{11}u \\ -m_{11}ur - d_{22}v \\ -(m_{22} - m_{11})u_i v - d_{33}r \end{bmatrix}, \quad (29)$$

and the observer of the USV is designed as

$$\begin{aligned} M\dot{\bar{V}} &= -D(V)V - C(V)V + \tau + \Delta, \\ \dot{\bar{\tau}}_d &= -b_2 \text{sign}(\bar{\tau}_d - \Delta), \end{aligned} \quad (30)$$

where $\Delta = -b_1 |M(\bar{V} - V)|^{\frac{1}{2}} \text{sign}(M(\bar{V} - V) + \bar{\tau}_d)$, $b_1, b_2 > 0$ are constant coefficients, $\bar{V} = [\bar{u}, \bar{v}, \bar{r}]^T$ is the estimate of the velocity vector $V = [u, v, r]^T$, and $\bar{\tau}_d = [\bar{\tau}_{ud} \ \bar{\tau}_{vd} \ \bar{\tau}_{rd}]^T$ is the estimate of the unknown time-varying disturbance vector $\tau_d = [\tau_{ud} \ \tau_{vd} \ \tau_{rd}]^T$.

Theorem 2 For the unknown time-varying disturbances τ_d in the USV dynamic model (0.3), they can be estimated by the designed observer (0.30) within a finite time.

Proof Let

$$\begin{aligned} \Omega &= M(\bar{V} - V), \\ \tilde{\tau}_d &= \bar{\tau}_d - \tau_d, \end{aligned} \quad (31)$$

and differentiate with respect to time, considering variables Ω and $\tilde{\tau}_d$,

$$\begin{aligned} \dot{\Omega} &= M(\dot{\bar{V}} - \dot{V}) \\ &= -D(V)V - C(V)V + \tau \\ &\quad - b_1 |M(\bar{V} - V)|^{\frac{1}{2}} \text{sign}(M(\bar{V} - V) + \bar{\tau}_d) \\ &\quad - (-C(V)V - D(V)V + \tau + \tau_d) \\ &= -b_1 |\Omega|^{\frac{1}{2}} \text{sign}(\Omega) + \bar{\tau}_d - \tau_d \\ &= -b_1 |\Omega|^{\frac{1}{2}} \text{sign}(\Omega) + \tilde{\tau}_d, \dot{\tilde{\tau}}_d = \dot{\bar{\tau}}_d - \dot{\tau}_d \\ &= -b_2 \text{sign}(\bar{\tau}_d - \tau_d - (\Delta - \tau_d)) - \dot{\tau}_d \\ &= -b_2 \text{sign}(\tilde{\tau}_d - \dot{\Omega}) - \dot{\tau}_d. \end{aligned} \quad (32)$$

According to assumption (2), the derivative of unknown time-varying disturbance $\dot{\tau}_d$ exists and is bounded. It can be concluded from (0.32) by using Lemma (3) that the states Ω and $\tilde{\tau}_d$ are finite-time stable. Thus, the estimator $\bar{\tau}_d$ converges to the actual disturbance τ_d within a finite time.

Based on the above analysis and proof, it can be known that when the velocities of the USV are the desired velocities (0.13), the USV network can ultimately achieve the optimal coverage of the task region \mathcal{Q} . Subsequently, a robust controller is designed for the USV to track the desired velocities (0.13) within a finite time while compensating for external disturbances.

Let $u_e = u - u_d$ be the error and $r_e = r - r_d$ be the error. The controller of the USV is designed as

$$\begin{bmatrix} \tau_u \\ 0 \\ \tau_r \end{bmatrix} = \begin{bmatrix} m_{11} \left[\frac{d_{11}}{m_{11}} u - \frac{m_{22}}{m_{11}} vr + \dot{u}_d + \nabla u \right] - \hat{\tau}_u \\ 0 \\ m_{33} \left[\frac{d_{33}}{m_{33}} r + \frac{m_{22} - m_{11}}{m_{33}} uv + \dot{r}_d + \nabla r \right] - \hat{\tau}_r \end{bmatrix}, \quad (33)$$

where $\begin{cases} \nabla u = -k_{\tau_u 1} \text{sig}^{\lambda_1(\xi_1)}(u_e) - k_{\tau_u 2} \text{sig}^{\eta_1(\varsigma_1)}(u_e), \\ \nabla r = -k_{\tau_r 1} \text{sig}^{\lambda_2(\xi_2)}(r_e) - k_{\tau_r 2} \text{sig}^{\eta_2(\varsigma_2)}(r_e), \end{cases}$ $k_{\tau_u 1}, k_{\tau_u 2}, k_{\tau_r 1}, k_{\tau_r 2} > 0$, $\text{sig}^r(s) = \text{sgn}(s)|s|^r$ and

$$\begin{cases} \lambda_1(\xi_1) = 1 + \xi_1(\frac{1}{2} + \frac{1}{2} \text{sgn}(|u_e| - 1)), \\ \eta_1(\varsigma_1) = 1 - \varsigma_1(\frac{1}{2} - \frac{1}{2} \text{sgn}(|u_e| - 1)), \end{cases} \tag{34}$$

$$\begin{cases} \lambda_2(\xi_2) = 1 + \xi_2(\frac{1}{2} + \frac{1}{2} \text{sgn}(|r_e| - 1)), \\ \eta_2(\varsigma_2) = 1 - \varsigma_2(\frac{1}{2} - \frac{1}{2} \text{sgn}(|r_e| - 1)), \end{cases} \tag{35}$$

$\xi_1 > 0, \xi_2 > 0$ and $0 < \varsigma_1 < \frac{1}{2}, 0 < \varsigma_2 < \frac{1}{2}$.

Theorem 3 Consider the USV dynamics described by (0.2) and (0.3), the designed control law (0.33) is capable of driving the velocities of USVs to track the desired velocities (0.13) within a finite time, and the optimal coverage effect of the task area Q can finally be achieved.

Proof Taking the derivative of time with respect to u_e , we can obtain

$$\begin{aligned} \dot{u}_e &= \dot{u} - \dot{u}_d \\ &= \frac{1}{m_{11}}(m_{22}vr - d_{11}u + \tau_u + \tau_{ud}) - \dot{u}_d \\ &= \frac{1}{m_{11}}(m_{22}vr - d_{11}u + m_{11}[\frac{d_{11}}{m_{11}}u \\ &\quad - \frac{m_{22}}{m_{11}}vr + \dot{u}_d + \nabla u] - \hat{\tau}_u + \tau_{ud}) - \dot{u}_d \\ &= \frac{1}{m_{11}}(m_{22}vr - d_{11}u + [d_{11}u - m_{22}vr \\ &\quad + m_{11}\dot{u}_d + m_{11}\nabla u] - \hat{\tau}_u + \tau_{ud}) - \dot{u}_d \\ &= \frac{1}{m_{11}}(m_{11}\dot{u}_d + m_{11}\nabla u - \hat{\tau}_u + \tau_{ud}) - \dot{u}_d \\ &= \dot{u}_d + \nabla u + \frac{1}{m_{11}}(\hat{\tau}_u - \tau_{ud}) - \dot{u}_d \\ &= \nabla u + \frac{1}{m_{11}}(\tau_{ud} - \hat{\tau}_u). \end{aligned} \tag{36}$$

According to Theorem 2, the observer’s estimate of the disturbances converges to the actual value of the disturbances in a finite time, which is denoted by T_1 . When $t > T_1$, one has

$$\begin{aligned} \dot{u}_e &= \nabla u \\ &= -k_{\tau_u 1} \text{sig}^{\lambda_1(\xi_1)}(u_e) - k_{\tau_u 2} \text{sig}^{\eta_1(\varsigma_1)}(u_e). \end{aligned} \tag{37}$$

When $|u_e| \geq 1$, Substituting (0.34) into (0.37) yields $\dot{u}_e = -k_{\tau_u 1} \text{sig}^{1+\xi_1}(u_e) - k_{\tau_u 2} \text{sig}(u_e)$. Let $y = |u_e|$, it can be obtained that $\dot{y} = -k_{\tau_u 1} y^{1+\xi_1} - k_{\tau_u 2} y$. When $|u_e| < 1$, Substituting (0.34) into (0.37) yields $\dot{u}_e = -k_{\tau_u 1} \text{sig}(u_e) - k_{\tau_u 2} \text{sig}^{1-\varsigma_1}(u_e)$. Let $y = |u_e|^{\varsigma_1}$, we can get $\dot{y} = -k_{\tau_u 1} \varsigma_1 y - k_{\tau_u 2} \varsigma_1$. Suppose error u_e starts at infinity ($y(0) \rightarrow \infty$). The time T_2 it takes for error u_e to converge from infinity to zero is

$$\begin{aligned} &\lim_{y(0) \rightarrow \infty} T_2(y(0)) \\ &= \lim_{y_0 \rightarrow \infty} (\int_0^1 \frac{1}{k_{\tau_u 1} \varsigma_1 y + k_{\tau_u 2} \varsigma_1} dy + \int_1^{y_0} \frac{1}{k_{\tau_u 1} y^{1+\xi_1} + k_{\tau_u 2} y} dy) \\ &= \frac{1}{k_{\tau_u 1} \varsigma_1} \ln(\frac{k_{\tau_u 1} + k_{\tau_u 2}}{k_{\tau_u 2}}) + \frac{1}{k_{\tau_u 2} \varsigma_1} \ln(\frac{k_{\tau_u 1} + k_{\tau_u 2}}{k_{\tau_u 1}}). \end{aligned} \tag{38}$$

So, it follows that the error u_e converges to 0 in time T_2 . The same analysis yields that the error r_e converges to 0 in time T_2 .

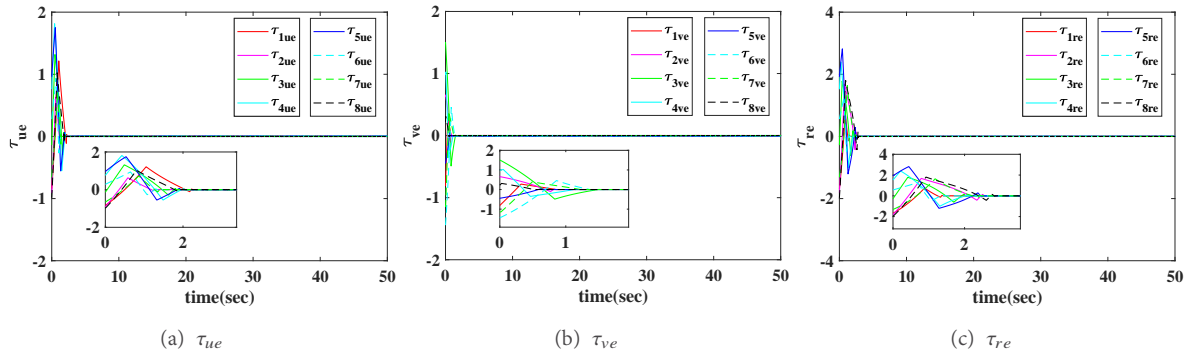


Figure 1. When the number of objects $m = 3$ and the number of USV $n = 8$, the curves of observation errors with time t for time-varying disturbances. USVs: unmanned surface vehicles.

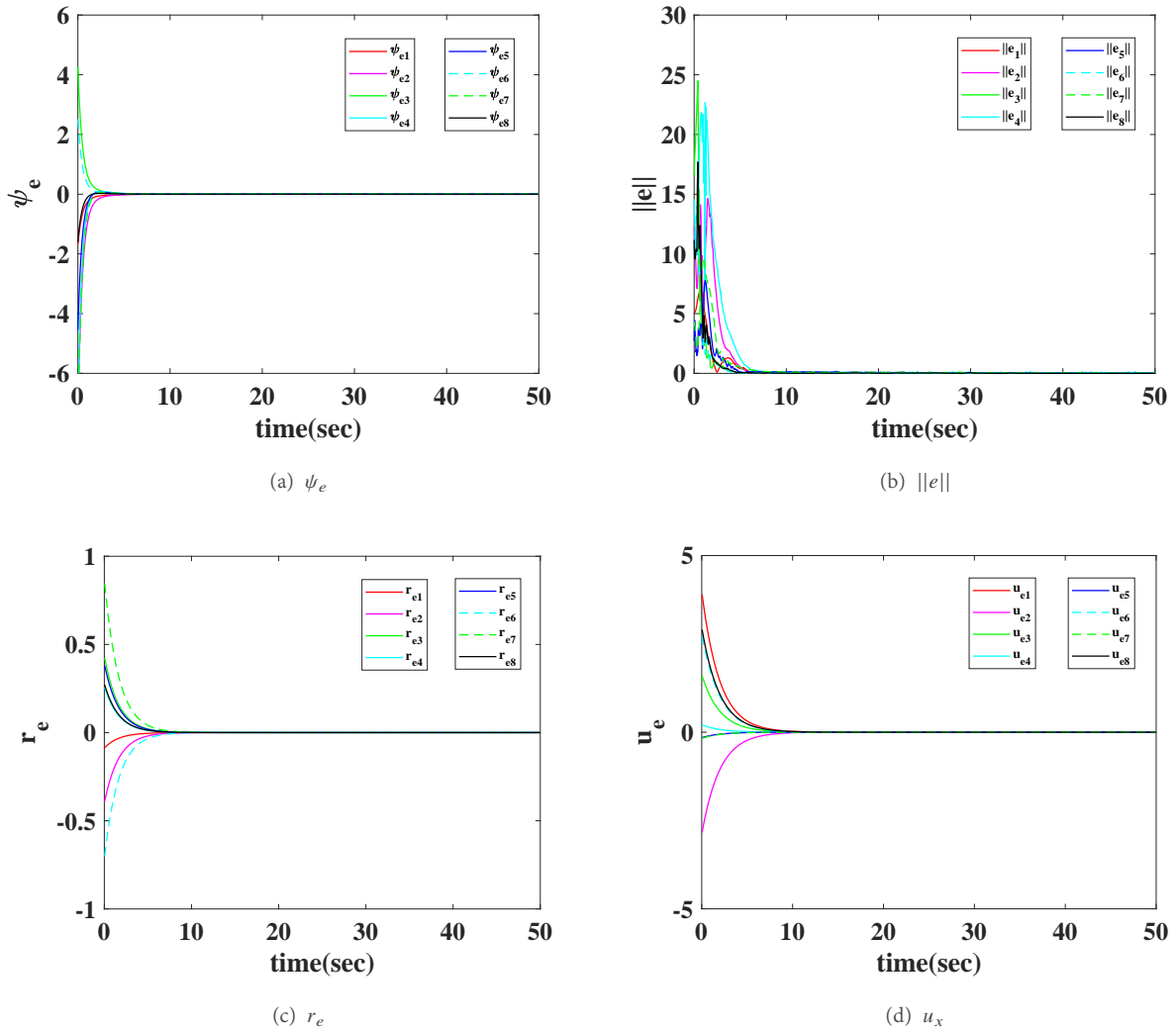


Figure 2. The curves of angular velocity error, surge velocity error, angle error, and distance error with time t .

It can be observed from theorem (2) that the designed observer (0.30) can estimate the external time-varying

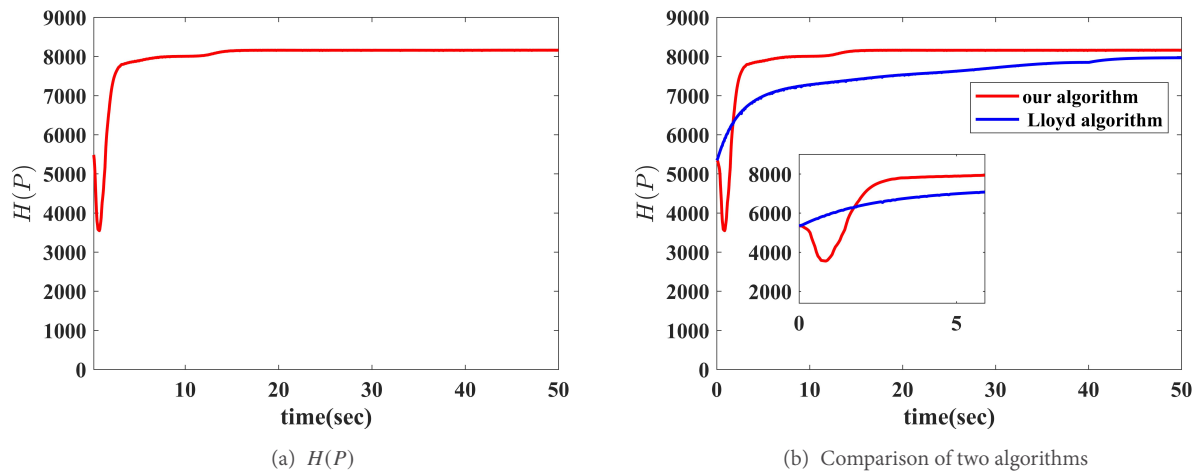


Figure 3. The curve of the metric function with time t (a), and comparison curve between our algorithm and traditional Lloyd algorithm (b).

disturbances within a finite time T_1 . Based on the above analysis, it can be concluded that the designed controller (0.33) can force the velocity error of the USV to converge to zero in T_2 after the external disturbance is estimated.

Therefore, the designed control law (0.33) can drive the velocities of the USV to track the desired velocities (0.13) within finite time $T_1 + T_2$. Therefore, when $t > T$, the velocities of the USV reach the expected velocities (0.13). Theorem (1) implies that maximizing the metric function (0.7) at the desired velocities (0.13) results in achieving optimal coverage of the task area Q .

Remark 2 The control law (0.33) contains the variable $\frac{d\hat{y}_{ir}}{dt}$, which exists and is bounded when $E \neq 0$. However, it has a singularity at $E = 0$. At the singularity, $E = 0$, the USV has achieved optimal coverage.

Remark 3 From the proof of theorem (3), it can be seen that the convergence time T_2 of the velocity errors is only related to the designed controller parameters $k_{\tau_{u1}}, k_{\tau_{u2}}, \varsigma_1, \varsigma_2$ and is independent of the initial state of the system. Thus, it is fixed time stable. However, considering the observation errors of the time-varying disturbances converge to zero within a finite time T_1 , the final conclusion is that the controller (0.33) forces velocity errors of the USV to converge to zero within a finite time $T_1 + T_2$.

5. SIMULATION RESULTS

In order to verify the disturbance observation method and USV coverage control method proposed in this paper, this section presents the simulation results for a scenario involving eight USVs ($n = 8$) and three important objects ($m = 3$). Consider a $100m \times 100m$ task area Q ; the risk density function is given by (0.5). The basic constant risk density $\phi(q) = 0.1$ and the contribution function $\phi_j(q, s_j)$ ($j = 1, 2, 3$) of objects to the risk density are defined as follows:

$$\begin{aligned} \phi_1(q, s_1) &= 10 \exp\left(-\frac{\|q-s_1\|^2}{200}\right), \\ \phi_2(q, s_2) &= 13 \exp\left(-\frac{\|q-s_2\|^2}{200}\right), \\ \phi_3(q, s_3) &= 8 \exp\left(-\frac{\|q-s_3\|^2}{200}\right). \end{aligned}$$

The kinematic and dynamic models of the USV are given by (0.1) and (0.3), respectively, and nominal physical parameters are as follows: $m_{11} = m_{22} = m_{33} = 2000, d_{11} = 20, d_{22} = 30, d_{33} = 35$. For the i -th USV ($i \in \mathcal{V}$),

the time-varying disturbances

$$\tau_d = \begin{bmatrix} \tau_{ud} \\ \tau_{vd} \\ \tau_{rd} \end{bmatrix} = \begin{bmatrix} \sin(t+i) \\ 1.5 \cos(t+i) \\ 2 \sin(t+i) \end{bmatrix},$$

and the initial positions and angles of the USVs are randomly assigned. It is assumed that each USV carries the actuator with the same performance, and the performance function is defined as:

$$f(\|q - p_i\|) = 0.5 \exp\left(-\frac{\|q - p_i\|^2}{1000}\right).$$

Firstly, the simulation results for observations of the time-varying disturbances are displayed in [Figure 1](#), where $\tau_{ue} = [\bar{\tau}_{1ud}, \bar{\tau}_{2ud}, \dots, \bar{\tau}_{8ud}] - [\tau_{1ud}, \tau_{2ud}, \dots, \tau_{8ud}]$ represents the observation error of the disturbance in surge velocity for each of the eight USVs, and τ_{ve} and τ_{re} are similar. It can be noted that the observation errors τ_{ue} , τ_{ve} , and τ_{re} converge to zero in finite time. This indicates that, under the designed disturbance vector observer, each USV effectively estimates the unknown time-varying disturbances, even though the input disturbances of each USV are time-varying and distinct.

Then, the simulation results of the angle errors and position errors at the desired velocities (0.13) are presented in [Figure 2\(a\)](#) and (b). These results indicate that each USV can drive the angle and position track the desired angle and position, respectively, at the expected velocities of the design.

The errors between the angular and surge velocities of each USV and the desired angular and surge velocities are shown in [Figure 2\(c\)](#) and (d). It can be clearly observed that the designed control law (0.33) can drive the velocities of each USV to track the desired velocities designed in (0.13), with external disturbances within the finite time.

Finally, the curves of the metric function (0.7) describing the coverage effect are shown in [Figure 3\(a\)](#), and the comparison between the algorithm designed in this paper and the classic Lloyd algorithm for optimizing regional coverage is shown in [Figure 3\(b\)](#). It is worth noting that the coverage optimization algorithm designed in this paper can achieve a superior coverage effect. Moreover, It is important to highlight that the coverage algorithm proposed in this paper is based on an underactuated USV model with disturbances, while the classic Lloyd algorithm is based on the first-order integral model robot. The coverage process of the USVs is illustrated in [Figure 4](#).

6. CONCLUSIONS

This paper proposes a method for observing unknown disturbances and an optimal coverage controller to address the challenge of region coverage control for a USV network. The proposed disturbance observation method is capable of estimating unknown time-varying disturbances within a finite time. Furthermore, a robust coverage controller is designed to enable the USV network to track the desired velocities within a finite time, achieving an optimal coverage effect of the task region. Simulation results demonstrate the effectiveness of the proposed approach. However, it is important to acknowledge that this paper has certain limitations. Specifically, it only considers simple convex task regions. If the task region is non-convex or contains obstacles, the coverage optimization control proposed in this paper may not be applicable. Therefore, future work will focus on addressing the challenges of collision avoidance and extending the coverage control problem to non-convex regions with obstacles.

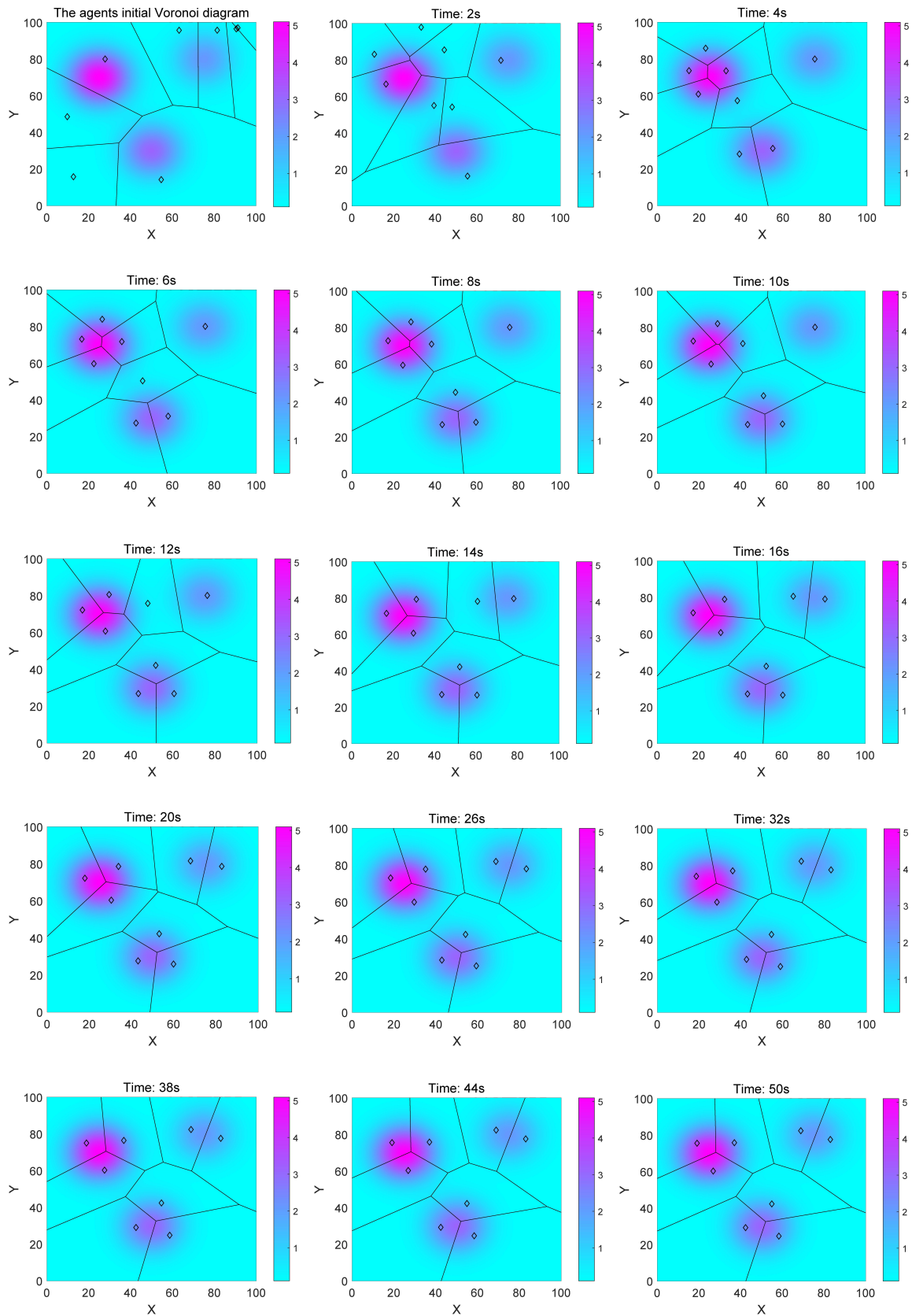


Figure 4. The coverage evolution process of the USVs to the task area, where the diamond represents the position of the USV, and different colors represent different risk density function values of the task area environment.

DECLARATIONS

Authors' contributions

Made significant contributions to the formal analysis and derivation of the content and has conducted the writing of the thesis and the completion of the first draft: Sun Q, Liu ZW

Contributed to the conceptualization of content, the review and editing of the article, and provided administrative, technical, and material support: Chi M, He D

Availability of data and materials

Not applicable.

Financial support and sponsorship

This work was supported by the National Natural Science Foundation of China under Grant 61973133.

Conflicts of interest

All authors declared that there are no conflicts of interest.

Ethical approval and consent to participate

Not applicable.

Consent for publication

Not applicable.

Copyright

© The Author(s) 2023.

REFERENCES

1. Liu ZW, Wen G, Yu X, Guan ZH, Huang T. Delayed impulsive control for consensus of multiagent systems with switching communication graphs. *IEEE Trans Cybern* 2019;50:3045-55. DOI
2. Xiao H, Cui R, Xu D. A sampling-based bayesian approach for cooperative multiagent online search with resource constraints. *IEEE Trans Cybern* 2017;48:1773-85. DOI
3. Xu JZ, Ge MF, Liu ZW, Zhang WY, Wei W. Force-reflecting hierarchical approach for human-aided teleoperation of NRS with event-triggered local communication. *IEEE Trans Ind Electron* 2021;69:2843-54. DOI
4. Miah S, Nguyen B, Bourque FA, Spinello D. Nonuniform deployment of autonomous agents in harbor-like environments. *Un Sys* 2014;2:377-89. DOI
5. Kantaros Y, Thanou M, Tzes A. Distributed coverage control for concave areas by a heterogeneous robot-swarm with visibility sensing constraints. *Automatica* 2015;53:195-207. DOI
6. Santos M, Diaz-Mercado Y, Egerstedt M. Coverage control for multirobot teams with heterogeneous sensing capabilities. *IEEE Robot Autom Lett* 2018;3:919-25. DOI
7. Rodríguez-Seda EJ, Xu X, Olm JM, Dòria-Cerezo A, Diaz-Mercado Y. Self-triggered coverage control for mobile sensors. *IEEE Trans Robot* 2023;39:223-38. DOI
8. Cortes J, Martinez S, Karatas T, Bullo F. Coverage control for mobile sensing networks. *IEEE Trans robot Automat* 2004;20:243-55. DOI
9. Stergiopoulos Y, Thanou M, Tzes A. Distributed collaborative coverage-control schemes for non-convex domains. *IEEE Trans Automat Contr* 2015;60:2422-27. DOI
10. Song C, Fan Y. Coverage control for mobile sensor networks with limited communication ranges on a circle. *Automatica* 2018;92:155-61. DOI
11. Miah S, Panah AY, Fallah MMH, Spinello D. Generalized non-autonomous metric optimization for area coverage problems with mobile autonomous agents. *Automatica* 2017;80:295-99. DOI
12. Dirafzoon A, Emrani S, Salehizadeh S, Menhaj MB. Coverage control in unknown environments using neural networks. *Artif Intell Rev* 2012;38:237-55. DOI
13. Schwager M, Rus D, Slotine JJ. Decentralized, adaptive coverage control for networked robots. *Int J Rob Res* 2009;28:357-75. DOI
14. Bai Y, Wang Y, Svinin M, Magid E, Sun R. Adaptive multi-agent coverage control with obstacle avoidance. *IEEE Control Syst Lett* 2021;6:944-49. DOI
15. Kwok A, Martinez S. Unicycle coverage control via hybrid modeling. *IEEE Trans Automat Contr* 2010;55:528-32. DOI
16. Sun Q, Chi M, Liu ZW, He D. Observer-based coverage control of unicycle mobile robot network in dynamic environment. *J Franklin Inst* 2022. DOI

17. Atinç GM, Stipanović DM, Voulgaris PG. A swarm-based approach to dynamic coverage control of multi-agent systems. *Automatica* 2020;112:108637. [DOI](#)
18. Park BS, Kwon JW, Kim H. Neural network-based output feedback control for reference tracking of underactuated surface vessels. *Automatica* 2017;77:353-9. [DOI](#)
19. Gonzalez-Garcia A, Castañeda H. Guidance and control based on adaptive sliding mode strategy for a USV subject to uncertainties. *IEEE J Oceanic Eng* 2021;46:1144-54. [DOI](#)
20. Zhang G, Chu S, Zhang W, Liu C. Adaptive neural fault-tolerant control for USV with the output-based triggering approach. *IEEE Trans Veh Technol* 2022;71:6948-57. [DOI](#)
21. Zhang G, Li J, Jin X, Liu C. Robust adaptive neural control for wing-sail-assisted vehicle via the multiport event-triggered approach. *IEEE Trans Cybern* 2022;52:12916-28. [DOI](#)
22. Li J, Zhang G, Shan Q, Zhang W. A novel cooperative design for USV-UAV Systems: 3D mapping guidance and adaptive fuzzy control. *IEEE Trans Control Netw Syst* 2023;10:564-74. [DOI](#)
23. Shang Y. Consensus seeking over Markovian switching networks with time-varying delays and uncertain topologies. *Appl Math Comput* 2016;273:1234-45. [DOI](#)
24. Shang Y. Median-based resilient consensus over time-varying random networks. *IEEE Trans Circuits Syst II* 2022;69:1203-7. [DOI](#)
25. Alvaro-Mendoza E, Gonzalez-Garcia A, Castañeda H, De León-Morales J. Novel adaptive law for super-twisting controller: USV tracking control under disturbances. *ISA Trans* 2023;S0019-2578(23)00196-3 [DOI](#)
26. Peng Z, Wang J, Wang D, Han QL. An overview of recent advances in coordinated control of multiple autonomous surface vehicles. *IEEE Trans Ind Inf* 2021;17:732-45. [DOI](#)
27. Arslan Ö. Statistical coverage control of mobile sensor networks. *IEEE Trans Robot* 2019;35:889-908. [DOI](#)
28. Shang Y. A system model of three-body interactions in complex networks: consensus and conservation. *Proc R Soc A* 2022;478:20210564. [DOI](#)
29. Ajina M, Tabatabai D, Nowzari C. Asynchronous distributed event-triggered coordination for multiagent coverage control. *IEEE Trans Cybern* 2020;51:5941-53. [DOI](#)
30. Kim S, Santos M, Guerrero-Bonilla L, Yezzi A, Egerstedt M. Coverage control of mobile robots with different maximum speeds for time-sensitive applications. *IEEE Robot Automa Lett* 2022;7:3001-7. [DOI](#)
31. An Q, Shen Y. Distributed coverage control for mobile camera sensor networks with anisotropic perception. *IEEE Sensors J* 2021;21:16264-74. [DOI](#)
32. Li WT, Liu YC. Human-swarm collaboration with coverage control under nonidentical and limited sensory ranges. *J Franklin Inst* 2019;356:9122-51. [DOI](#)
33. Drazin PG, Drazin PD. Nonlinear systems. *Cambridge University Press* 1992. [DOI](#)
34. Shtessel YB, Shkolnikov IA, Levant A. Smooth second-order sliding modes: missile guidance application. *Automatica* 2007;43:1470-76. [DOI](#)